

ELECTROCHEMICAL SO_x AND NO_x SENSORS WITH Ag⁺-β"-ALUMINA AS SOLID ELECTROLYTE AND Ag AS SOLID REFERENCE ELECTRODE

N. Rao (a), O.T. Sorensen (b), J. Schoonman and C.M. van den Bleek (a)

(a) Delft Univ. of Technology, NL-2600 GA Delft, The Netherlands

(b) Riso National Lab., DK-4000 Roskilde, Denmark

ABSTRACT

Polycrystalline Ag⁺-β"-Alumina tubes and pellets were prepared from Na⁺-β"-Alumina by ion exchange and characterized by XRD, DTA, TGA, SEM and EDAX analysis. Applying Ag⁺-β"-Al₂O₃ as solid electrolyte, metal Ag as solid reference electrode and porous Pt as working electrode, fully solid galvanic cells were constructed as SO_x and NO_x electrochemical sensors:

Pt, Ag/Ag⁺-β"-Al₂O₃/Ag₂SO₄/porous Pt, SO₂-SO₃-O₂, Pt
Pt, Ag/Ag⁺-β"-Al₂O₃/AgNO₃/porous Pt, NO₂-NO-O₂, Pt

The Nernst EMF response of the SO_x sensor to the SO₂ partial pressure is fairly consistent with the theoretical prediction in the working temperature region of 500-700°C and the pSO₂ range of 10 ppm to 1000 ppm. The response time is usually about 5-10 mins. The experimental results indicate the potential of this SO_x sensor in practical use. A primary investigation of NO_x sensors shows that the sensor has promising EMF response to the change of NO partial pressure from 500 ppm to 1000 ppm in the operating temperature range of 150-220°C, but the response time is as long as a few hours, which might be shortened by improving the properties of Pt working electrode.

1. INTRODUCTION

It is of great importance to develop a reliable and rapid method for the continuous measurement of the SO_x ($x=2,3$) and NO_x ($x=1,2$) concentrations in the atmosphere and gaseous environments of industrial processes. For these measurements, solid state electrochemical sensors with solid electrolytes have advantages over other detection methods.

Since the first SO_x sensor with solid electrolyte was reported by Gauthier et al [1,2], many attempts have been made to use alkali sulfates including K_2SO_4 [1,2], Na_2SO_4 [3] and $\text{Li}_2\text{SO}_4\text{-Ag}_2\text{SO}_4$ two phases solid solution [4] as solid electrolytes for SO_x sensors. However, these alkali metal sulfates undergo phase transition with volume change on heating and have poor sinterability. This would result in micro cracks and pores. In recent years, some Na^+ ion conductors such as Nasicon [5], β, β'' -Alumina [6] were employed to avoid the above problems because no structural phase transition takes place during heating from room temperature to the melting point of these materials. But, a standard gas reference with a known SO_2 partial pressure is necessary when a galvanic cell with a Na^+ conductor is used as an SO_x sensor. Considering the ion exchangability of Na^+ - β'' -Alumina by other ions, in our previous work [7], we prepared polycrystalline Ag^+ - β'' -Alumina and used it as the solid electrolyte. In this case, metal Ag is a good choice as the stable solid reference for a fully solid SO_x sensor. Itoh et al [8] also published the similar work on the Ag^+ - β - Al_2O_3 sensor disks. The present paper is focused on our recent experimental results for the SO_2 sensor with a tubular Ag^+ - β'' -alumina solid electrolyte.

Regarding NO_x sensors, two types of material were applied, one is semiconductor, such as metal oxides [9,10,11] and phthalocyanines [12], the other is solid electrolyte, e.g. nitrates [13] and $\text{Na-}\beta/\beta''\text{-Al}_2\text{O}_3$ [14]. Semiconductor sensors usually have the problem of selectivity. For the solid electrolyte sensors being developed, there is also a problem of choosing a good solid reference. In this work, a primary study on NO_x sensors with $\text{Ag-}\beta''$ -alumina as solid electrolyte, metal Ag as solid reference and porous Pt as working electrode is being carried out.

2. EXPERIMENTAL

Polycrystalline Na⁺-β"-Alumina tubes (φ11x1.5x40) and pellets (φ16x1.5, φ10x1) used in this work were supplied by Shanghai Institute of Ceramics, Academia Sinica. To obtain Ag⁺-β"-Alumina, Na⁺-β"-Alumina samples were dipped into a molten AgNO₃ at 300°C to undergo ion exchange reaction for 30 hrs. The ion exchange completeness of the Na⁺ by Ag⁺ was examined with the weight increase of the samples, Na⁺ content of the samples after ion exchange was detected by EDAX.

The XRD patterns of the specimens were taken on a D/max-ra 12kw Diffractometer (Rikadenki, Japan) over the 2θ range from 20° to 70°. An X-650 SEM (Hitachi, Japan) was used to obtain the surface morphology of the sensor material. DTA and TG were employed to investigate the thermal stability of the materials by a DF-30 Thermoanalyzer (Shimadzu, Japan).

Using Ag⁺-β"-Alumina as solid electrolyte, metal Ag as solid reference electrode and porous Pt as working electrode, the tubular SO_x and both planar and tubular NO_x sensors were fabricated. Figure 1 shows the SO_x sensor tube and the electrodes, the SO_x sensors were tested in a system shown in figure 2. The sample gas with different SO_x partial pressure was made by mixing air and SO₂ in N₂. As can be seen, two mass flow meters were employed to control the gas flow rate and the SO₂ partial pressure on the working electrode. NO_x sensor device has a similar construction. The Nernst EMF response and working temperature of the SO_x and NO_x sensors were collected by an HP 85B PC or a recorder, then analysed using Supercalc 4 program. EMF response as a function of operating time, SO₂, NO and O₂ partial pressure and working temperature were tested respectively.

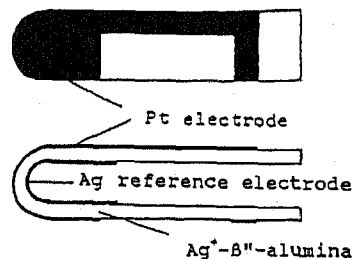


Fig.1 Ag⁺-β"-alumina SO₂ sensor tube and electrodes.

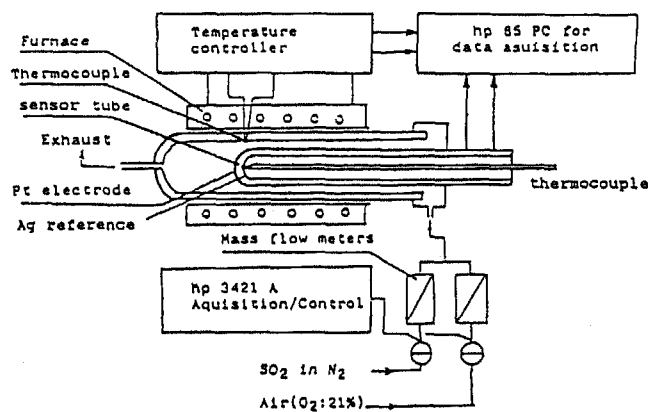


Fig.2 System for the testing of $\text{Ag}^+\text{-}\beta''\text{-alumina}$ SO_2 sensors.

3.RESULTS AND DISCUSSION

3.1 Preparation and characterization of $\text{Ag}^+\text{-}\beta''\text{-Alumina}$

The measurement on the weight increase of the $\text{Na}^+\text{-}\beta''\text{-alumina}$ samples after ion exchange showed that at 300°C in AgNO_3 melt, the complete ion exchange of Na^+ by Ag^+ in $\beta''\text{-alumina}$ could be accomplished in less than 30 hrs. XPS, EPMA and X-ray fluoroscopy analysis all indicated that no Na^+ ion could be detected in the sample after 30 hrs of ion exchange.

Figure 3 gives an SEM photo showing a typical microstructure of the polycrystalline $\text{Ag}^+\text{-}\beta''\text{-Al}_2\text{O}_3$. XRD pattern indicated that $\text{Ag}^+\text{-}\beta''\text{-Al}_2\text{O}_3$ has the same lattice structure as $\text{Na}^+\text{-}\beta''\text{-Al}_2\text{O}_3$. $\text{Ag}^+\text{-}\beta''\text{-Alumina}$ exhibits good thermal stability as $\text{Na}^+\text{-}\beta''\text{-alumina}$, there is no phase transition from room temperature to 1200°C . Furthermore, $\text{Na}^+\text{-}\beta''\text{-Alumina}$ is easily corroded by CO_2 and/or H_2O , forming Na_2CO_3 or NaHCO_3 while $\text{Ag}^+\text{-}\beta''\text{-Alumina}$ is quite stable in moist air. Even when the $\text{Ag}^+\text{-}\beta''\text{-Alumina}$ samples were put into water for 10 hrs and then analyzed, no considerable changes were observed in their structure and properties. The good chemical

stability of Ag⁺-β"-alumina makes it easy to be used in practical environment.

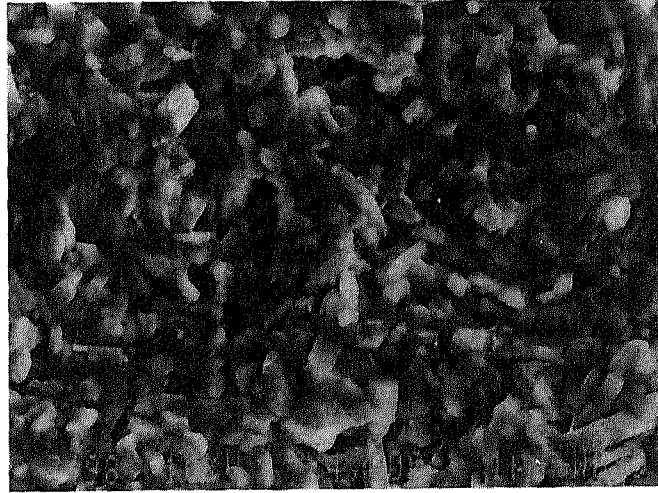
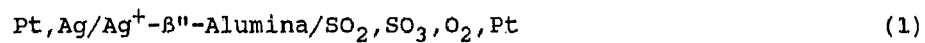


Fig.3 SEM photo showing a typical microstructure of Ag⁺-β"-alumina

3.2 EMF expression for the Ag⁺-β"-Al₂O₃ SO_x and NO_x sensors
For the following galvanic cell



The theoretical EMF of this cell can be expressed as

$$\text{EMF} = -\Delta G^\circ(T)/2F + (RT/2F) * \ln[K\text{PO}_2 / (1 + K\text{PO}_2^{1/2})] + (RT/2F) * \ln\text{PSO}_2 \quad (2)$$

where $\Delta G^\circ(T)$ is the standard free energy of the cell reaction



and K is the equilibrium constant for the reaction



$\Delta G^\circ(T)$ and K can be calculated from the thermodynamic data:

$$\Delta G^\circ (600\text{K} < T < 703\text{K}) = -312148 + 227.36T \quad (\text{J/mol}) \quad (5)$$

$$\Delta G^\circ (703\text{K} < T < 933\text{K}) = -290016 + 196.10T \quad (\text{J/mol}) \quad (6)$$

$$\Delta G^\circ (933\text{K} < T < 1100\text{K}) = -261600 + 165.52T \quad (\text{J/mol}) \quad (7)$$

and

$$\ln K (600\text{K} < T < 1100\text{K}) = -11.15 + 11783/T \quad (8)$$

In equation (2), PSO_2 is the initial SO_x ($x=2,3$) partial pressure in the gas mixture introduced into the sensor system. If PO_2 is known (Say, 0.21 atm for atmosphere), PSO_2 could be calculated from the measured EMF of the sensor cell. Figure 4 and 5 show the theoretical EMF as a function of SO_2 concentration and temperature, respectively. We can see that EMF increases with SO_2 partial pressure but decreases with temperature. When temperature is rather high and SO_3 concentration is very small, for instance, at the fixed temperature, PSO_3 is below its decomposition partial pressure for reaction(3), the theoretical EMF calculation will give negative values, and it implies that the electrochemical reaction is stopped.

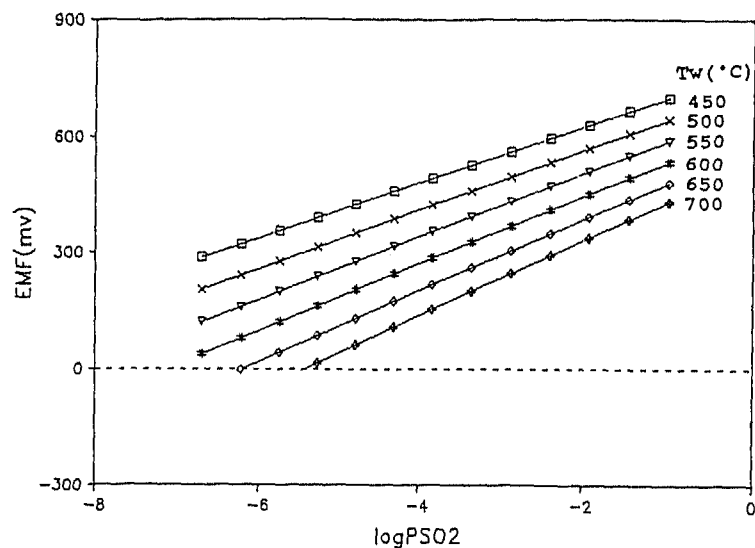


Fig.4 Theoretical EMF of the Ag^+-B'' -alumina as a function of SO_2 partial pressure when $PO_2=0.21\text{atm}$.

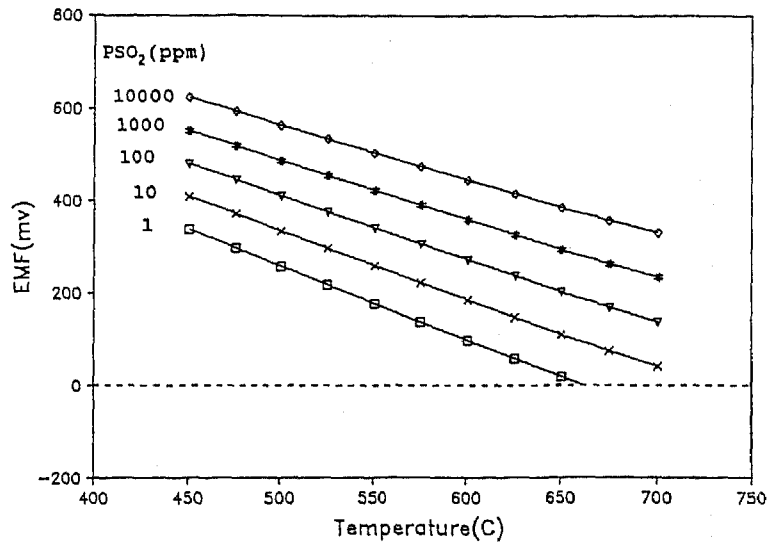


Fig.5 Theoretical EMF of the Ag⁺-β"-alumina SO₂ sensor as a function of temperature when PO₂=0.21atm.

In this case, the formed Ag₂SO₄ on the working electrode will completely decompose to silver metal, SO₃ and O₂ gas, and this sensor cell cannot work anymore, the EMF output of this sensor should become zero. Therefore, in practical measurements, the working temperature should be controlled to avoid the decomposition of Ag₂SO₄.

For NO_x sensors, a similar theoretical discussion can be given and theoretical EMF can be predicted by the equations below

$$EMF = -\delta G^\circ(T)/F + RT/F \cdot \ln[KP(O_2)/(1 + KP(O_2)^{1/2})] + RT/F \cdot \ln P(NO) \quad (9)$$

$$\delta G^\circ(298K < T < 433K) = -152130 + 239.6T \quad (J/mol) \quad (10)$$

$$\delta G^\circ(433K < T < 483K) = -145578 + 224.5T \quad (J/mol) \quad (11)$$

$$\delta G^\circ(483K < T < 600K) = -131871 + 196.4T \quad (J/mol) \quad (12)$$

and

$$\ln(K) = -9.15 + 6993/T \quad (13)$$

3.3 EMF response to SO₂ partial pressure

Figure 6(a) shows the sensor EMF response to the change of SO₂ partial pressure from 30ppm to 140ppm at the working temperature of 615°C. We can see that the response time is about 5-10 mins, at low SO₂ partial pressure, the response time is longer and the EMF

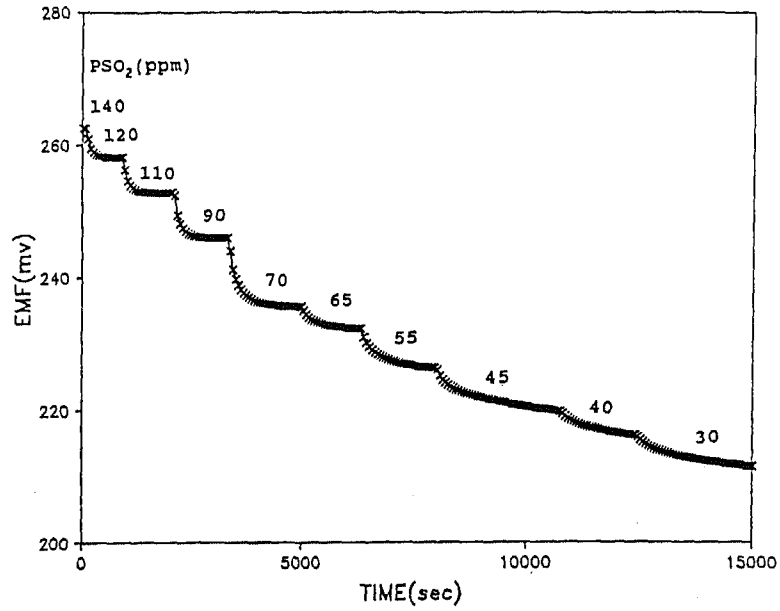


Fig.6(a) Sensor EMF response to the change of SO_2 concentration when $T_w = 615^\circ C$.

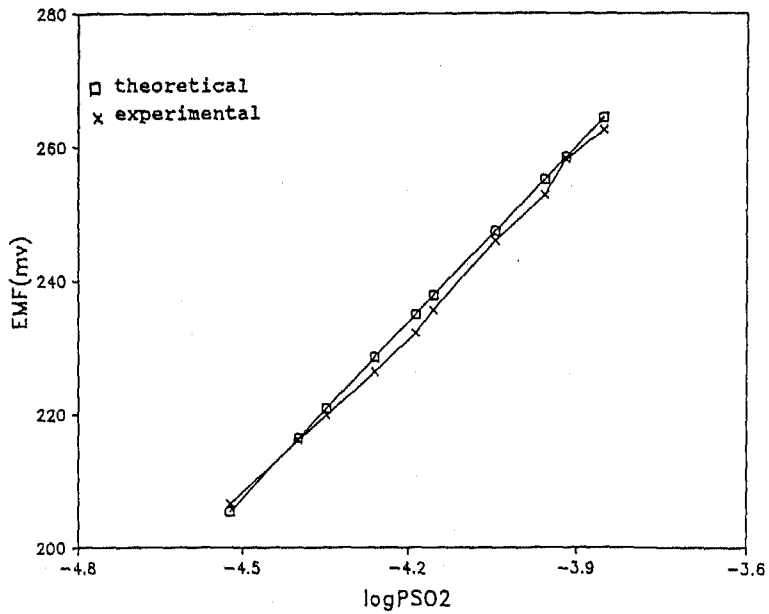


Fig.6(b) EMF response as a function of SO_2 concentration when $T_w = 615^\circ C$.

value decreases slightly. Figure 6(b) gives the EMF response as a function of SO₂ partial pressure calculated from Figure 6(a). It can be seen that the EMF values are essentially consistent with the theoretical prediction from equation (2), a little negative deviation of the experimental results from the theoretical values could be attributed to the lack of the catalytic activity of the Pt electrode for reaction (4). An SO₃ partial pressure smaller than the equilibrium value certainly leads to a lower EMF response of the sensor.

Figure 7(a) shows an EMF response curve similar to figure 6(a) at the same working temperature but higher SO₂ partial pressure. A sharp increase of the EMF response can be observed when the SO₂ concentration increases, but when the SO₂ concentration changes to a smaller value, the EMF response is slower. It might be caused by the difficulty of the SO₂/SO₃ gas escape from the Pt electrode. Figure 7(b) shows the SO₂ dependence of the sensor EMF response calculated from figure 7(a). Here we also see the experimental EMF in good agreement with the predicted value.

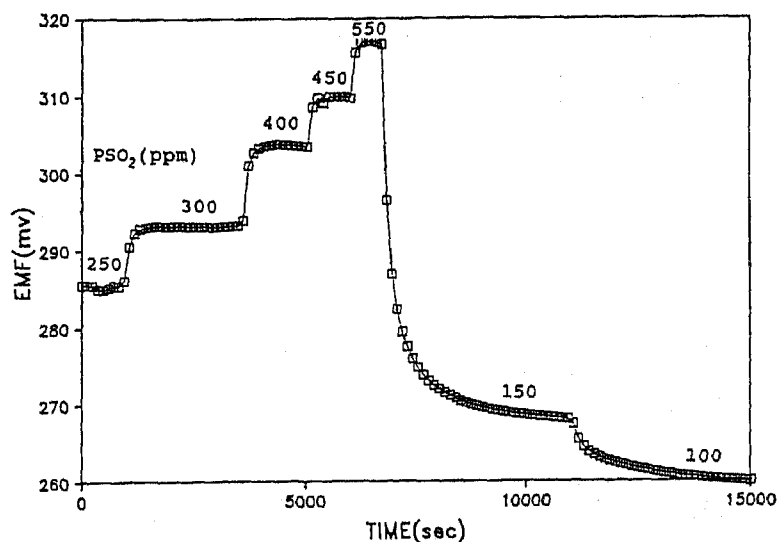


Fig.7(a) Sensor EMF response to the change of SO₂ concentration when Tw=615°C.

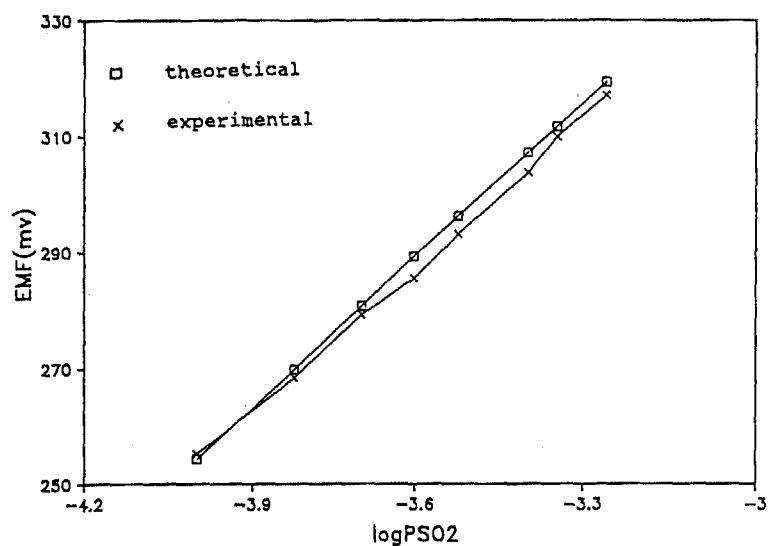


Fig.7(b) EMF response as a function of PSO₂ when Tw=615°C.

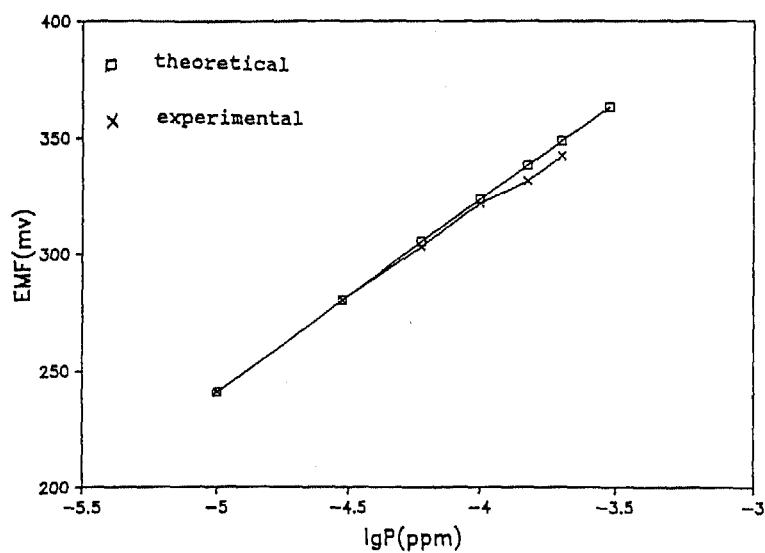


Fig.8 EMF response as a function of SO₂ partial pressure when Tw=565°C

Figure 8 gives another EMF response as a function of SO₂ partial pressure at the working temperature of 565°C. As is seen, the experimental EMF value fits the theoretical value quite well in the low SO₂ concentration range, however, a negative deviation was observed at high SO₂ concentration.

3.4 Temperature dependence of sensor response

The curves shown in figure 9 are the theoretical and experimental temperature dependence of the sensor EMF response when P_{SO₂}=10ppm. Obviously, from 500°C to 700°C, the experimental EMF values are in excellent agreement with the theoretical ones at higher temperatures, while in the low temperature range, a negative deviation of the EMF output was observed. It may be because that the porous Pt electrode as catalyst is not enough for the equilibrium of SO₂ oxidation. If some other catalyst such as V₂O₅ can be used upstream in the gas system, the sensor response at low temperature could be improved.

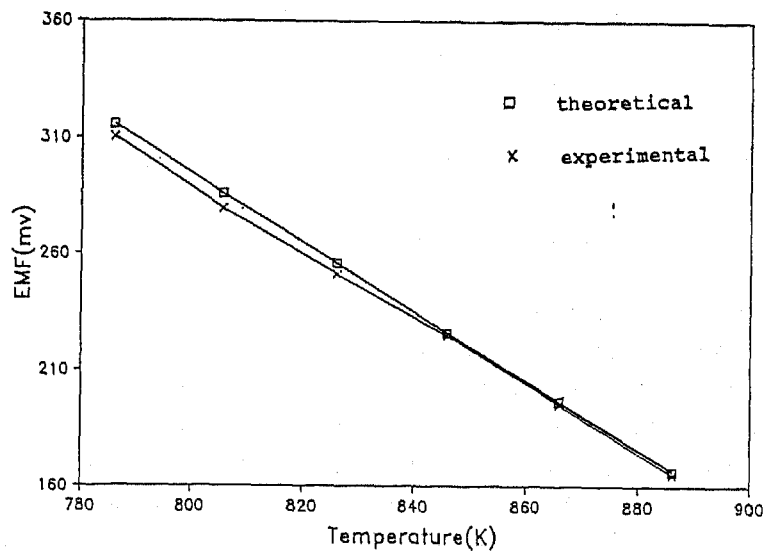


Fig.9 Temperature dependence of the sensor response when P_{SO₂}=10ppm.

Figure 10 shows another example of temperature dependence of the sensor EMF response when $PSO_2=100\text{ppm}$. We can see that the experimental EMF fits the theoretical value quite well. Similar results were also obtained for other SO_2 concentrations in the range of $PSO_2=10-1000$ ppm.

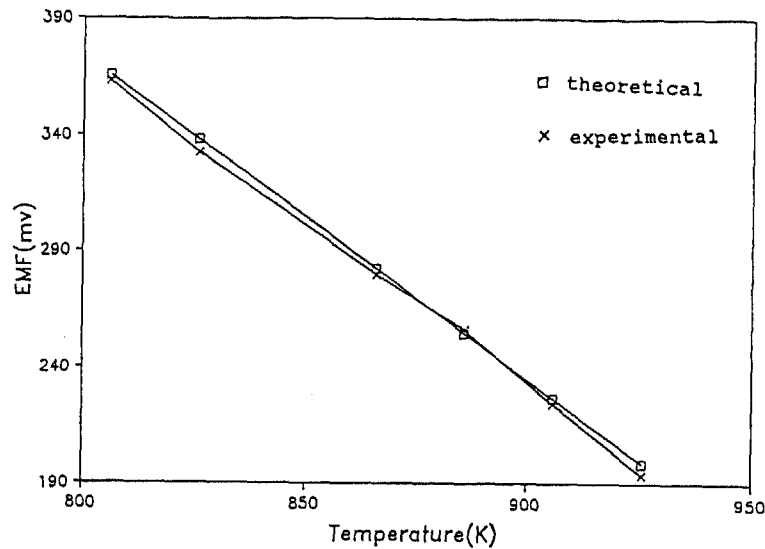


Fig.10 EMF response as a function of temperature when $PSO_2=100\text{ppm}$.

3.5 NO_x sensors EMF response

Two planar Ag- β "-alumina NO_x sensors are being tested. It took a few hours to form a $AgNO_3$ layer in pure NO_2 and after that a constant EMF signal of about 420 mV was obtained at 150°C . Then a gas mixture of Ar, O_2 and NO was introduced into the system and it has been seen that EMF signal sensitively increases when NO concentration is higher. At 200°C , when NO concentration is around 500-1000 ppm and O_2 partial pressure is about 15%, an EMF response within 300 mV can be observed. However, it takes as long as a couple of hours to get a stable response which may result from the low operating temperature. Two tubular NO_x sensors are also to be tested.

Based on the above results, it is clear that this Ag⁺-β"-alumina SO_x sensor could be developed by improving the catalytic activity of the porous Pt working electrode and it has prospect of commercial use. However, for NO_x sensors, the study has been just started and further efforts should be made to get improvement.

4. CONCLUSIONS

(1) Ag⁺-β"-Alumina polycrystalline materials were prepared from Na⁺-β"-Alumina by ion exchange reaction at 300°C in the AgNO₃ melt. It has a typical polycrystalline surface morphology and the same lattice structure as Na⁺-β"-Al₂O₃. Its chemical stability is better than Na⁺-β"-Al₂O₃ which will make it easily used in practical measurements.

(2) Fully solid state SO_x sensor with a tubular Ag⁺-β"-alumina as solid electrolyte, silver metal as solid reference electrode and porous Pt as working electrode was fabricated in gas flowing system. When the temperature is higher than 500°C and the SO₂ concentration is in the range of 10-1000 ppm, the EMF output of the sensor shows a good Nernst response consistent with the theoretical prediction, and the response time is usually about 5-10 mins. The experimental results indicate the potential of this SO₂ sensor in practical use.

(3) A preliminary study on planar and tubular Ag-β"-alumina NO_x sensors has been started.

ACKNOWLEDGEMENTS

The authors would like to thank Mr. K.G.Chen of Shanghai Institute of Ceramics, Academia Sinica for his supplying of Na⁺-β"-Alumina materials and Mr. H.Jensen of PBI-Development Dansensor for his help in the fabrication of the sensor device. We also want to give our thanks to Mr. P.V.Jensen, Mr. C.Klitholm, Mr. H.Nilsson of Riso National Lab. and Mr. B.Meester of Delft University of Technology for their kind assistance.

REFERENCES

1. Gauthier, M. and Chamberland, A.: J. Electrochem. Soc., 1977, 124, 1579
2. Gauthier, M.: J. Electrochem. Soc., 1977, 124, 1584
3. Jacob, K.T. and Rao, D.R.: J. Electrochem. Soc., 1979, 126, 1842
4. Worrell, W.L. and Liu, Q.G.: Sens. Actu., 1982, 2, 385
5. Maruyama, T.; Saito, Y.; Mastumoto, Y. and Yano, Y.: Solid State Ionics, 1985, 17, 286
6. Itoh, M. and Kozuka, Z.: Trans. Jpn. Inst. Mat., 1986, 26, 1
7. Meng, G.; Shen, G.; Rao, N.; Peng, D. and Lin, Z.: J. Sensor Techn., 1989, 2, 17
8. Itoh, M. and Kozuka, Z.: J. Electrochem. Soc., 1986, 133, 1512
9. Ishihara, T.; Shiokawa, K.; Eguchi, K. and Arai, H.: Sens. Actu., 1989, 19, 259
10. Ishihara, T.; Shiokawa, K.; Eguchi, K. and Arai, H.: Chem. Lett., 1988, 997
11. Sberveglieri, G. and Groppelli, S.: Sens. Actu., 1988, 15, 235
12. Bott, B. and Jones, A.: Sens. Actu., 1984, 5, 43
13. Yanagida, H.: Euro. Pat. Appl., EP 0 182 921 A1
14. Hotzel, G. and Weppner, W.: Proc. 2nd. Int. Con. Chem. Sens., 1986, 285